A new $k - \varepsilon - \gamma$ model

F. Miralles

IMAG, Université de Montpellier

14 septembre 2022

Introduction

- Flow past a circular cylinder

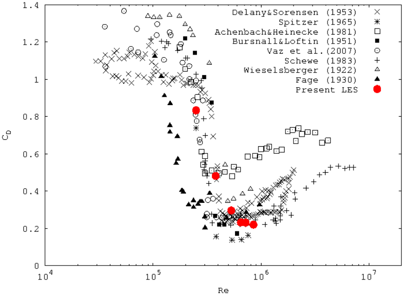

Figure – Drag crisis [?]

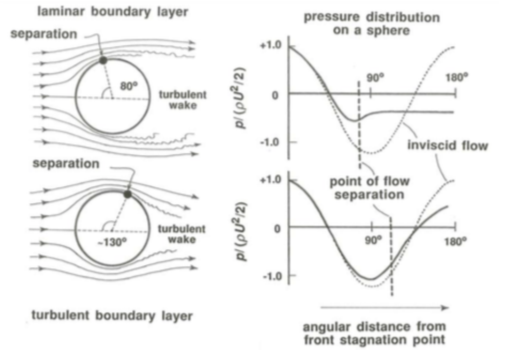

Figure – Illustrate picture of flow separation

- Akhter 2015 transitional model using $\varepsilon = \beta^* \omega k$, equations can be transformed in :

$$\frac{\partial \rho\gamma}{\partial t} + \nabla \cdot \rho \mathbf{u}\gamma = \underbrace{C_{g1}\gamma(1-\gamma)\frac{P_k}{k}}_{Production} + \underbrace{\rho C_{g2}\frac{k^2}{\varepsilon}\nabla\gamma\cdot\nabla\gamma}_{Auxiliary\ production} \tag{1}$$

$$+ \nabla \cdot \underbrace{[\sigma_\gamma(1-\gamma)(\mu+\mu_t)\nabla\gamma]}_{\mathcal{D}_\gamma} \tag{2}$$

with $C_{\mu g} = 10^{-7} = c_{\mu g}(\beta^*)^2$ and the turbulent viscosity

$$\mu_t^* = \left[1 + C_{\mu g}\frac{k^3}{\varepsilon^2}\gamma^{-2}(1-\gamma)\|\nabla\gamma\|^2\right] c_\mu f_\mu \frac{k^2}{\epsilon} \tag{3}$$

- Initial and boundary condition :

$$\gamma_{\partial C} = 1, \quad \text{and } \gamma_\infty = 0.01 = \gamma(\mathbf{x}, 0) \quad \forall \mathbf{x} \in \Omega_f$$

Name	Mesh size	y_w^+	$\overline{C}_d$	C_l'	$-\overline{C}_{pb}$	L_r	$\overline{\theta}$
Present simulation							
URANS $k-\varepsilon$	0.6M	1	0.50	0.24	0.51	1.00	109
URANS $k-\varepsilon-\gamma$	0.6M	1	0.51	0.23	0.49	1.10	110

Table – Bulk coefficient of the flow around a circular cylinder at Reynolds number 1M

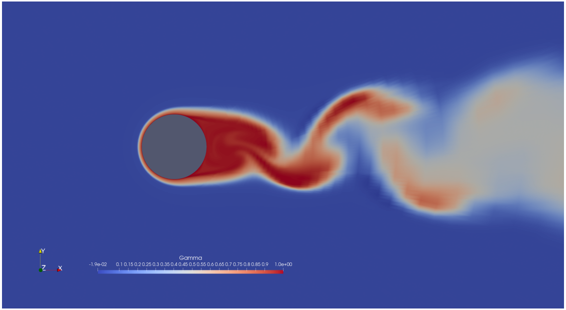

Figure – Gamma field

- Why the model does not work ?
  - idea 1) Too much production : the production term must be defined with the shear stress
$$P_\gamma = \mu_t^* \frac{\partial \mathbf{u}}{\partial y}$$
the production term related variation of velocity with body topology.
  - idea 2) $\gamma = 1$ on the boundary means that the flow is completely turbulent, replaced by Neumann B.C
$$\nabla\gamma \cdot \mathbf{n} = 0$$
γ must be free on the boundary.
  - idea 3) Gamma influence on others variables is too small, modify the turbulent viscosity is not sufficient. We propose the following k equation based on the transitional Menter model :
$$\frac{\partial \rho k}{\partial t} + \nabla \cdot (\rho \mathbf{u} k) = \max(\gamma, \alpha_1) P_k - \max(\gamma, \alpha_2) D_k + \nabla \cdot [(\mu + \mu_t \sigma_k) \nabla k]$$

■ Problem Averaged Navier-Stokes compressible equations with $k - \varepsilon$ closure model :
Find $(\rho, \rho\mathbf{u}, \rho E, \rho k, \rho\epsilon, \rho\gamma)$ solution of :

$$\begin{cases} \dfrac{\partial \rho k}{\partial t} + \nabla\cdot(\rho\mathbf{u}k) = \max(\gamma,\alpha_1)P_k + \nabla\cdot[(\mu+\mu_t\sigma_k)\nabla k] - \max(\gamma,\alpha_2)D_k, \\ \dfrac{\partial \rho\varepsilon}{\partial t} + \nabla\cdot(\rho\mathbf{u}\varepsilon) = \left(c_\varepsilon^{(1)}\tau : \nabla\mathbf{u} - c_\varepsilon^{(2)}\rho\varepsilon + C^{(2)}\right)\dfrac{1}{T(k,\varepsilon)} + \nabla\cdot[(\mu+\mu_t\sigma_\varepsilon)\nabla\varepsilon] \\ \dfrac{\partial \rho\gamma}{\partial t} + \nabla\cdot(\rho\mathbf{u}\gamma) = C_{g1}\gamma(1-\gamma)\dfrac{P_\gamma}{k} + \rho C_{g2}\dfrac{k^2}{\varepsilon}\nabla\gamma\cdot\nabla\gamma \\ \qquad\qquad + \nabla\cdot[\sigma_\gamma(1-\gamma)(\mu+\mu_t^*)\nabla\gamma] \end{cases} \tag{4}$$

with $\mu_t^* = \left[1 + C_{\mu g}\frac{k^3}{\varepsilon^2}\gamma^{-2}(1-\gamma)\|\nabla\gamma\|^2\right] c_\mu f_\mu \frac{k^2}{\epsilon}$ and $P_k = \tau : \nabla\mathbf{u}$ and $D_k = \rho\varepsilon$.

- Parameter α_1 and α_2
  - $\alpha_1 = 0.5$ deal with the production term
  - $\alpha_2 = 0.1$ deal with the destruction term

- Approximate viscous jacobian matrix of turbulent model :

$$\begin{pmatrix} 0 & 1 & 0 \\ \frac{1}{T(k,\varepsilon)} & 2\frac{c_\varepsilon^{(2)}}{T(k,\varepsilon)} & 0 \\ 0 & 0 & \frac{\partial \mathcal{P}_\gamma}{\partial \rho\gamma} \end{pmatrix} \tag{5}$$

- Approximation of the γ jacobian source term on a tetrahedron :

$$\left.\frac{\partial \mathcal{P}_{\gamma,h}}{\partial \rho\gamma}\right|_T \simeq C_{g1} \overline{\frac{1}{\rho_h k_h}(1-2\gamma_h)}^T P_k \tag{6}$$

$$\left(\left.\frac{\partial \mathcal{D}_{\gamma,h}}{\partial \rho\gamma}\right|_T\right)_i \simeq \sigma_\gamma \left(\mu + \overline{\mu_t}^T\right)\left[(1-\overline{\gamma_h}^T)\sum_{j=1}^{4}\frac{1}{\rho_j}\frac{\partial \phi_j}{\partial \mathbf{x}_i} - \overline{\left(\frac{1}{\rho}\right)_h}^T \sum_{j=1}^{4}\gamma_j\frac{\partial \phi_j}{\partial \mathbf{x}_i}\right] \tag{7}$$

- **Set up**
  - Mach $= 0.1$,
  - regime :

$$\begin{cases} \text{sub-critical } Re = 3900 \\ \text{supercritical } Re = 1M \\ \text{transcritical } Re = 2M \end{cases}$$

  - $U_\infty = 34.025$, $\rho_\infty = 1.225$
  - turbulence intensity : $I_k = 0.5\%$
  - $k_\infty = \frac{3}{2}\left(I_k U_\infty\right)^2$, $\varepsilon_\infty = k_\infty/10$

- **Boundary conditions** :

$$\nabla\gamma \cdot \mathbf{n}_{\partial C} = 0, \quad \text{and } \gamma_\infty = 0.01$$

- **Mesh** : $y_w^+ = 1 \Leftrightarrow \delta = 4 \times 10^{-5}$

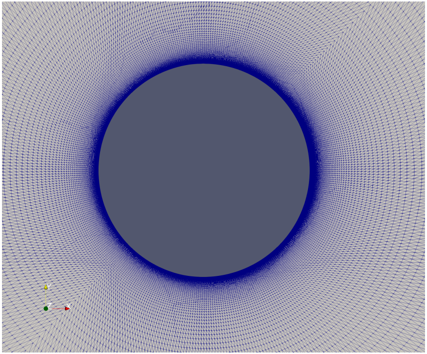

Figure – Radial mesh

Name	Mesh size	$\overline{C}_d$	C_l'	$-\overline{C}_{pb}$	L_r	$\overline{\theta}$	St
Present simulation							
$k-\varepsilon-\gamma$	176K	0.97	0.17	0.78	1.68	89	0.21
$k-\varepsilon$ Goldberg	176K	0.96	0.11	0.85	1.56	111	0.20
$k-R$	176K	1.00	0.11	0.86	1.53	93	0.20
Numerical simulation							
Spalart 3D [Abalakin et al., 2019]	-	0.97	0.11	0.83	1.67	89	0.21
DVMS WALE 3D [Moussaed et al., 2014]	1.46M	0.94	-	0.85	1.47	-	0.22
Experiment							
[Norberg, 1994]	-	0.94-1.04	-	0.84-0.93	-	-	0.20
[Parnaudeau et al., 2008]	-	-	0.1	-	1.41-1.58	-	-
[?]	-	-	-	-	-	86	-

Table – Bulk coefficient of the flow around a circular cylinder at Reynolds number 3900, $\overline{C}_d$ holds for the mean drag coefficient, $\overline{C}_l'$ is the root mean square of lift time fluctuation, $\overline{C}_{p_b}$ is the pressure coefficient at cylinder basis, L_r is the mean recirculation length, $\overline{\theta}$ is the mean separation angle.

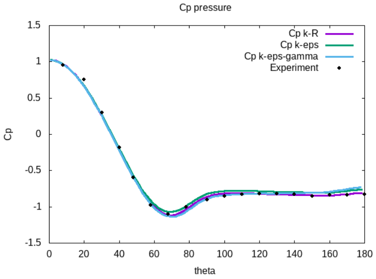

Figure – Meanflow pressure distribution at Re = 3900

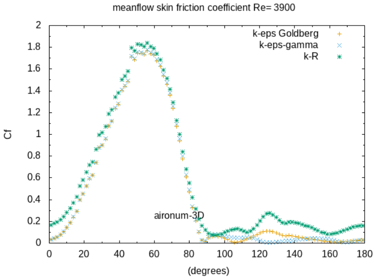

Figure – Meanflow skin friction distribution at Re = 3900

Name	Mesh size	y_w^+	$\overline{C}_d$	C_l'	$-\overline{C}_{pb}$	L_r	$\overline{\theta}$
Present simulation							
URANS $k-\varepsilon$	**0.6M**	**1**	**0.50**	**0.24**	**0.51**	**1.00**	**109**
DDES $k-\varepsilon$ **Goldberg ITW**	**4.8M**	**1**	**0.50**	**0.07**	**0.54**	**1.22**	**103**
k - ε **/ cubic WALE ITW**	**4.8M**	**1**	**0.48**	**0.11**	**0.55**	**1.14**	**109**
URANS $k-\varepsilon-\gamma$	**0.6M**	**1**	**0.27**	**0.0**	**0.20**	**0.47**	**134**
URANS $k-\varepsilon-\gamma$**/ DVMS**	**0.6M**	**1**	**0.30**	**0.10**	**0.31**	**0.90**	**140**
URANS $k-\varepsilon-\gamma$**/ DVMS WALE**	**0.6M**	**1**	**0.31**	**0.12**	**0.33**	**0.80**	**130**
Experiments							
[Shih et al., 1993a]			**0.24**	**-**	**0.33**		
[Schewe, 1983]			**0.25**	**-**	**0.32**		
[Gölling, 2006]						**-**	**130**
[Zdravkovich, 1997]			**0.2-0.4**	**0.1-0.15**	**0.2-0.34**		

Table – Bulk coefficient of the flow around a circular cylinder at Reynolds number 1M, $\overline{C}_d$ holds for the mean drag coefficient, C_l' is the root mean square of lift time fluctuation, $\overline{C}_{p_b}$ is the pressure coefficient at cylinder basis, L_r is the mean recirculation length, $\overline{\theta}$ is the mean separation angle.

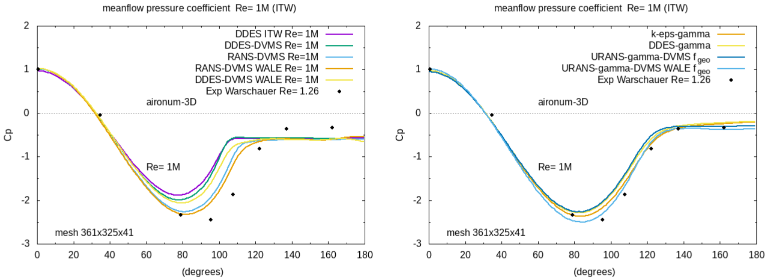

Figure – Integration to the wall meanflow pressure distribution, without transitional model on left side, within $k - \epsilon - \gamma$ model on right side

- The blending function that we choose writes :

$$\theta = 1 - f_\delta \left(1 - \tanh\left(\frac{\Delta_T}{k^{3/2}}\varepsilon\right)\right) \quad (8)$$

$$f_\delta = \exp\left(-\frac{1}{\epsilon_0}\min(\delta - d, 0)^2\right), \quad \varepsilon_0 > 0 \text{ small} \quad (9)$$

- Which value of δ ?

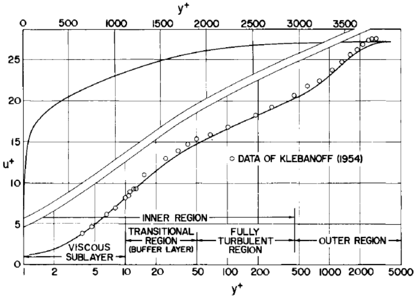

Figure – Boundary layer [Wilcox, 1994]

- δ can be chosen as the end of turbulent boundary layer :

$$\delta = \frac{Y^+ Re}{20} \quad (10)$$

- with $Y^+ = 500$

- As we can see, larger $Y+$ is, damped are the fluctuations :

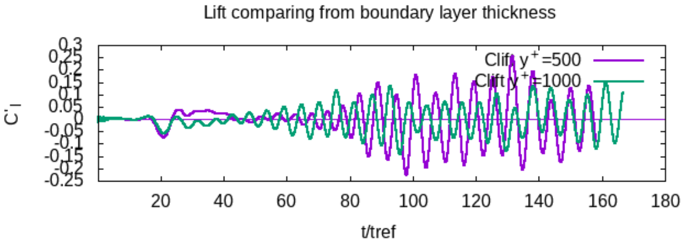

Figure – Graphs of the lift coefficient fluctuation, comparison with two boundary layer thickness in hybrid run.

- Skin friction coefficient using Achenbach definition :

$$C_f = \frac{\overline{\tau_w}}{1/2\rho_\infty U_\infty^2}\sqrt{Re}, \quad \text{with } \tau_w \text{ the mean value of wall shear stress} \qquad (11)$$

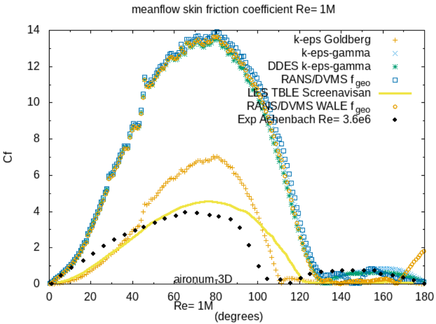

Figure – Distribution of skin friction coefficient as a function of polar angle. Comparison between experiment.

	Mesh	$\overline{C}_d$	C_l'	$-\overline{C_{pb}}$	$\overline{\theta}$	St
Present simulation						
URANS $k-\varepsilon$	0.6M	0.52	0.25	0.60	111	-
URANS $k-\varepsilon$/DVMS WALE	0.6M	0.48	0.27	0.60	109	-
URANS $k-\varepsilon-\gamma$	0.6M	0.25	0.0	0.19	130	-
URANS $k-\varepsilon-\gamma$/DVMS WALE	0.6M	0.25	0.03	0.26	135	-
Other simul.						
LES/ TBLE [Sreenivasan and Kannan, 2019]		0.24	0.029	0.36	105	-
Measurements						
Exp. [Shih et al., 1993b]		0.26	0.033	0.40	105	
Exp. [Schewe, 1995]		0.32	0.029	-		

Table – Bulk coefficients of the flow around a circular cylinder at Reynolds number 2×10^6.

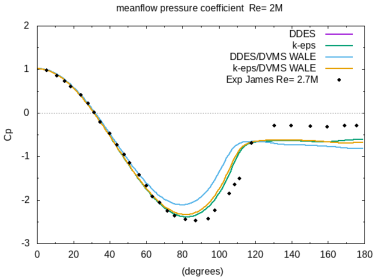

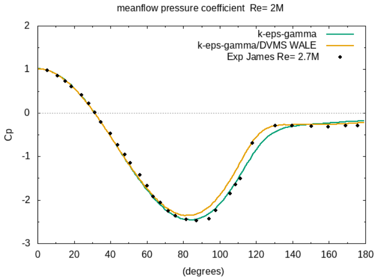

Figure – Integration to the wall meanflow pressure distribution, without transitional model on left side, within $k - \epsilon - \gamma$ model on right side

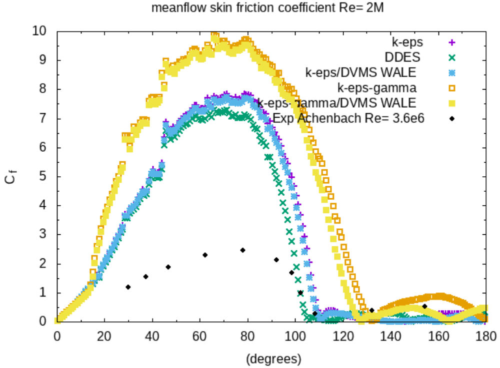

Figure – Distribution of skin friction coefficient as a function of polar angle. Comparison between experiment.

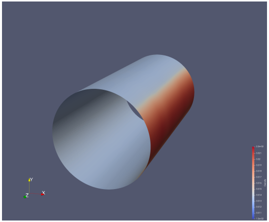

Figure – Gamma distribution on cylinder surface.

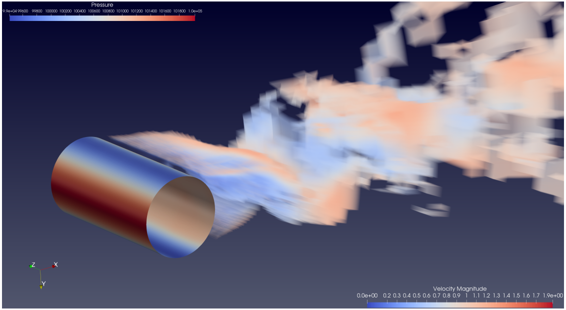

Figure – Separation of the fluid flow.

- Conclusion and summary
  - We shown a new transition model
  - It provide a good behavior in sub-critical case
  - In super critical flow, pressure distribution and separation of boundary layer are in good agreement with experiment
  - But the lift is not caught, it need to be blend with LES-like model
  - In order to be efficient, θ must be 0 where $y^+ > 500$, else lift coefficient is dissipated by RANS effect

Abalakin, I., Duben', A., Zhdanova, N., and Kozubskaya, T. (2019).
Simulating an unsteady turbulent flow around a cylinder by the immersed boundary method.
Mathematical Models and Computer Simulations, 11 :74–85.

Gölling, B. (2006).
Experimental investigations of separating boundary-layer flow from circular cylinder at reynolds numbers from 105 up to 107.
pages 455–462.

Moussaed, C., Wornom, S., Salvetti, M. V., Koobus, B., and Dervieux, A. (2014).
Impact of dynamic subgrid-scale modeling in variational multiscale large-eddy simulation of bluff-body flows.
Acta Mechanica, 225 :3309–3323.

Norberg, C. (1994).
An experimental investigation of the flow around a circular cylinder : influence of aspect ratio.
Journal of Fluid Mechanics, 258 :287–316.

Parnaudeau, P., Carlier, J., Heitz, D., and Lamballais, E. (2008).
Experimental and numerical studies of the flow over a circular cylinder at reynolds number 3900.
Physics of Fluids, 20(8) :085101.

Schewe, G. (1983).
On the force fluctuations acting on a circular cylinder in crossflow from subcritical up to transcritical reynolds number.